

Controlling optical gain in semiconducting polymers with nanoscale chain positioning and alignment

IGNACIO B. MARTINI¹, IAN M. CRAIG¹, WILLIAM C. MOLENKAMP¹, HIROKATSU MIYATA², SARAH H. TOLBERT^{1*} AND BENJAMIN J. SCHWARTZ^{1*}

¹Department of Chemistry and Biochemistry, University of California, Los Angeles, California 90095-1569, USA

²Canon Research Center, Leading-Edge Technology Development Headquarters, Canon Inc. 3-30-2 Shimomaruko, Ohta-ku Tokyo, 146-8501 Japan

*e-mail: tolbert@chem.ucla.edu; schwartz@chem.ucla.edu

Published online: 16 September 2007; doi:10.1038/nnano.2007.294

We control the chain conformation of a semiconducting polymer by encapsulating it within the aligned nanopores of a silica host. The confinement leads to polarized, low-threshold amplified spontaneous emission from the polymer chains. The polymer enters the porous silica film from only one face and the filling of the pores is therefore graded. As a result, the profile of the index of refraction in the film is also graded, in the direction normal to the pores, so that the composite film forms a low-loss, graded-index waveguide. The aligned polymer chains plus naturally formed waveguide are ideally configured for optical gain, with a threshold for amplified spontaneous emission that is twenty times lower than in comparable unoriented polymer films. Moreover, the optimal conditions for ASE are met in only one spatial orientation and with one polarization. The results show that nanometre-scale control of semiconducting polymer chain orientation and position leads to novel and desirable optical properties.

Conjugated polymers are remarkable materials that combine the optical and electronic properties of semiconductors with the mechanical properties and processing advantages of plastics¹. Although these materials are often thought of as homogeneous low-cost organic analogues to inorganic semiconductors, in this work we show that their unique one-dimensional polymeric nature provides for new applications that are not available with traditional inorganic semiconductors. Specifically, we take advantage of the fact that the optical properties of these one-dimensional organic semiconductors are not isotropic, but rather are highly polarized along the chain axis². As a result, physical alignment of the polymer chains results in alignment of their transition dipoles³, which in turn leads to new and interesting optical properties. Here, we focus on amplified spontaneous emission (ASE), the cavityless cousin of lasing⁴. We find that spatially aligning the conjugated polymer chains on nanometre length scales by encapsulation in an ordered nanoporous silica film^{5–10} leads to the production of directional, highly polarized ASE with a low excitation threshold. Although directionality and polarization are common in lasing, it is generally an external cavity that imposes such constraints. However, in this work, we accomplish these characteristics by controlling the nanometre-scale spatial position of the polymer chains using host–guest chemistry^{11–13}. This allows us both to achieve alignment by molecularly orienting the polymer chromophores and to provide optical feedback by spatially distributing the polymer chromophores to form a low-loss, graded-index waveguide.

To achieve polymer alignment, we confine the polymer chains within surfactant-templated nanoporous silica hosts^{5,6}. Such hosts can be formed by co-assembling silica precursors with

organic surfactants to produce structures reminiscent of lyotropic liquid crystals with the solvent phase replaced by crosslinked silica. Subsequent removal of the surfactant template produces controlled, periodic nanoporous materials. Although a wide range of nanoscale architectures can be produced^{14,15}, the hexagonal honeycomb phase is particularly interesting because it contains long, straight pores with tunable pore diameter. Thin films of these hosts can be formed from solution by means of hydrothermal⁷ or evaporation-based methods⁸. In both cases, the pores tend to lie in the plane of the film to optimize favourable interactions with the substrate. It has also been shown that if such films are grown on a rubbed polyimide substrate, uniaxial in-plane pore alignment can be achieved^{9,10}. Such oriented pores provide new opportunities for using spatial confinement to control the electronic properties of semiconducting polymers.

Previous work by the authors has established that spatial confinement of semiconducting polymers in templated nanoporous silicas can be used to generate optical materials with unique properties, including control over emission polarization^{3,11}, energy transfer^{12,16} and the density of defect sites. More importantly for this work, we have also shown that with the proper choice of pore size, both chain conformation and aggregation can be controlled to produce arrays of close-packed, straight polymer chains¹³. Despite these advantages, encapsulation of semiconducting polymers in nanoporous hosts has not yet found an application for lasing, even though the use of semiconducting polymers as the active medium for plastic lasers is well established^{4,17,18}. The large optical cross-sections, high density of chromophores and relatively low optical losses of conjugated polymers can lead either to ASE when the light is

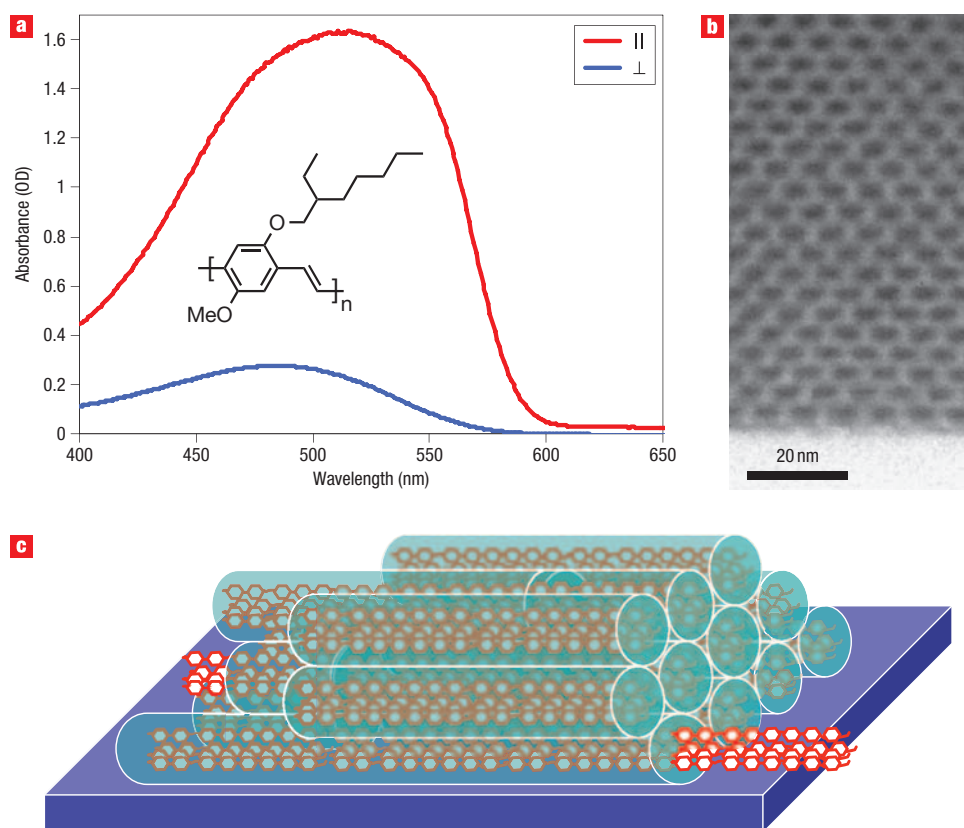


Figure 1 Composite films of aligned silica nanopores containing the semiconducting polymer poly(2-methoxy-5-(2'-ethyl-hexyloxy)-1,4-phenylene vinylene) (MEH-PPV). **a**, The UV-visible absorption spectrum of a typical MEH-PPV/aligned mesoporous silica composite film for light polarized parallel (\parallel) and perpendicular (\perp) to the pore direction; the inset shows the chemical structure of MEH-PPV. **b**, TEM image of a thin section of a typical aligned nanoporous silica film. **c**, Schematic of conjugated polymer chains incorporated into the aligned nanoporous silica channels.

confined in the natural waveguide formed by a spin-cast polymer film⁴, or to lasing when optical feedback is provided by an external microcavity¹⁷ or in-plane distributed feedback¹⁸. In this report, we show how controlling both the conformation and the physical position of the polymer chains on the nanoscale produces dramatic improvements in the ability of conjugated polymers to undergo optical gain without the need for externally imposed optical feedback.

For this work, optical-quality, aligned silica–polymer composite samples were created using hydrothermal methods to produce oriented nanoporous silica films, followed by diffusive incorporation of the semiconducting polymer poly(2-methoxy-5-(2'-ethyl-hexyloxy)-1,4-phenylene vinylene) (MEH-PPV; ref. 19) into the pores. Figure 1b shows a transverse electron microscopy (TEM) image of the highly aligned, highly periodic silica nanopores, and Fig. 1c illustrates schematically how the polymer chains incorporate into these pores. For all the optical measurements presented in this work, the film was covered with a layer of glycerol sandwiched inside a second glass slide. To measure the ability of our polymer–silica composite films to undergo stimulated emission, we excited the samples using polarized laser pulses of ~ 120 fs duration tuned to the 500-nm absorption maximum of MEH-PPV (ref. 20). Emission from the edge of the films was collected through a polarizer and spectrally analysed with a polychromator and charge-coupled device (CCD). We also studied the ASE behaviour of spin-cast films of pure MEH-PPV and blends of MEH-PPV in polystyrene (PS). To measure the

optical gain and loss in our samples, we used a cylindrical lens to excite stripes of different lengths at different positions from the edge of the films²¹. To refer to the orientations of the sample and the polarizations of the light in our experiments, we describe each experiment with three indices. The first index indicates whether or not the polarization of the excitation laser is parallel (\parallel) or perpendicular (\perp) to the pore direction; the second index describes whether the light emitted in the plane of the film was collected along (\parallel) or against the pore direction (\perp); and the third index specifies whether the polarization of the collected light was parallel (\parallel) or perpendicular (\perp) to the plane of the substrate.

Figure 1a shows the polarized absorption of MEH-PPV incorporated into the aligned mesoporous silica films. The absorption spectra are shown on an absolute scale; the factor of ~ 6 difference at 500 nm between absorption polarized along the pore direction (\parallel , red curve) versus polarized perpendicular to the pore direction (\perp , blue curve) verifies that the polymer chromophores are predominantly aligned along the pore direction. This alignment also gives rise to highly polarized emission¹¹, which forms the basis for the unique optical gain effects observed here. Figure 2 shows intensity-dependent emission spectra from MEH-PPV/silica composite samples for a variety of polarization combinations. Although the final narrowed linewidth is limited by the resolution of our spectrometer, the sharp spectral narrowing of the emission at high excitation fluences in the $\parallel, \perp, \parallel$ polarization combination (Fig. 2a) is the classic signature of ASE, indicating that optical

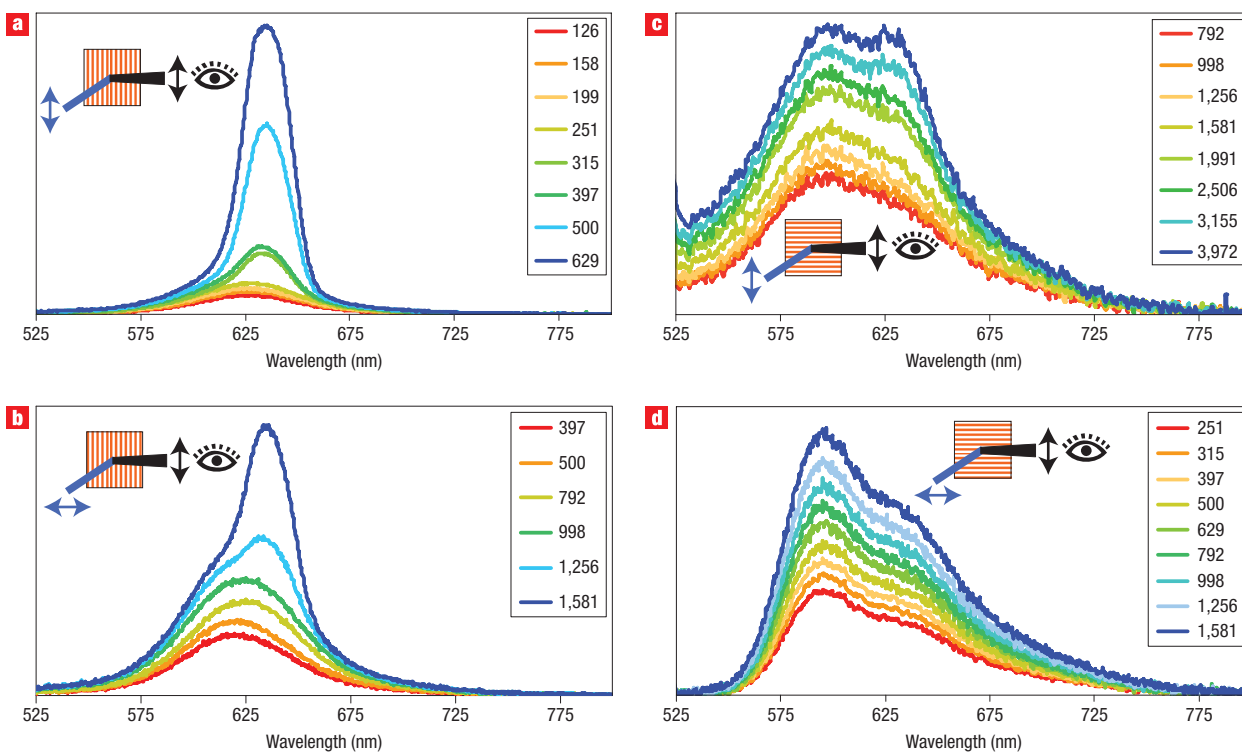


Figure 2 Intensity-dependent emission spectra from an MEH-PPV/aligned mesoporous silica composite film. **a–d**, Images are shown for four of the eight possible sample alignment/polarization combinations: $\parallel, \perp, \parallel$ (**a**); \perp, \perp, \parallel (**b**); $\perp, \parallel, \parallel$ (**c**); and $\parallel, \parallel, \parallel$ (**d**). The first index indicates whether the polarization of the 500-nm excitation laser was parallel (\parallel) or perpendicular (\perp) to the pore direction; the second index describes whether the light emitted in the plane of the film was collected along (\parallel) or against the pore direction (\perp); and the third index specifies whether the polarization of the collected light was parallel (\parallel) or perpendicular (\perp) to the plane of the substrate. The excitation fluence for each measurement is indicated in nJ mm^{-2} . Line narrowing was not observed for the four polarization combinations that are not shown, similar to $\parallel, \parallel, \parallel$ and $\perp, \parallel, \parallel$.

gain by means of stimulated emission is taking place⁴. The amplified light is emitted along the plane of the film only in the direction perpendicular to the pores; no narrowing is observed in either the $\parallel, \parallel, \perp$ (not shown) or $\parallel, \parallel, \parallel$ geometries (Fig. 2d).

To make comparison easier, the upper panel of Fig. 3 shows ASE thresholds, plotted as that the fraction the emission spectrum has narrowed (measured at the full-width half-maximum, FWHM) versus the excitation fluence. For the $\parallel, \perp, \parallel$ case (grey diamonds), the emission is 50% narrowed at $\sim 300 \text{ nJ mm}^{-2}$. By contrast, for the $\perp, \parallel, \parallel$ and $\parallel, \parallel, \perp$ combinations, no line narrowing is observed even at intensities of $\sim 5 \mu\text{J mm}^{-2}$, the highest we could apply without damaging the sample. Although the optical density (OD) of the sample is ~ 6 times higher for \parallel excitation than for \perp excitation (compare with Fig. 1a), the amount of absorbed excitation light is identical for the $\parallel, \perp, \parallel$ and the $\parallel, \parallel, \perp$ or $\parallel, \parallel, \parallel$ geometries. The data thus indicate that the ASE threshold for non-optimal geometries, such as $\parallel, \parallel, \perp$ or $\parallel, \parallel, \parallel$, is at least 13 times higher, and likely orders of magnitude higher than that for the $\parallel, \perp, \parallel$ combination. Clearly, the difference in ASE threshold is not simply an OD effect; rather, it results from the high degree of alignment of the polymer chains in the composite, which makes it impossible for the chromophores to build up gain when the emitted light is not polarized parallel to the pores.

Figure 2b shows intensity-dependent emission spectra from the composites for the \perp, \perp, \parallel polarization combination. Even though the excitation polarization is against the pore direction, line narrowing is still observed because the emission

direction and polarization are both favourable for ASE. The black circles in Fig. 3a show that the ASE threshold for this polarization combination is roughly five times higher than for the $\parallel, \perp, \parallel$ combination, similar to the difference in OD between the two samples. In contrast, the difference in steady-state emission intensity between these samples is only approximately a factor of three, indicating that perpendicular excitations can easily reorient to produce parallel emission, either through energy transfer¹² or through excited-state relaxation that rotates the direction of the emission transition dipole.

Overall, the data in Figs 2 and 3a show that it is the orientation of the polymer chains, not the polarization of the excitation laser, which determines the directionality of stimulated emission and gain in the composite MEH-PPV/silica films. Moreover, the data show clearly that ASE can be controlled by pore orientation; the ASE threshold can be modulated by a factor of ~ 5 using the polarization of the excitation laser (for example, $\parallel, \perp, \parallel$ versus \perp, \perp, \parallel), or line narrowing can be switched off using a fixed excitation intensity either by rotating the sample (for example, $\parallel, \perp, \parallel$ versus $\perp, \parallel, \parallel$) or by changing the spatial position of the detector (for example, $\parallel, \perp, \parallel$ versus $\parallel, \parallel, \parallel$ or $\parallel, \parallel, \perp$).

In addition to providing control over ASE, the encapsulation and alignment of the polymer chains in the mesoporous silica films also provides the advantage of lowering the ASE threshold by over a factor of 20 relative to spin-cast polymer films. Figure 3b shows ASE threshold plots for the $\parallel, \perp, \parallel$ polarization geometry from a composite sample (black diamonds) and for a 28% w/w blend spin-cast film of MEH-PPV in PS (grey squares).

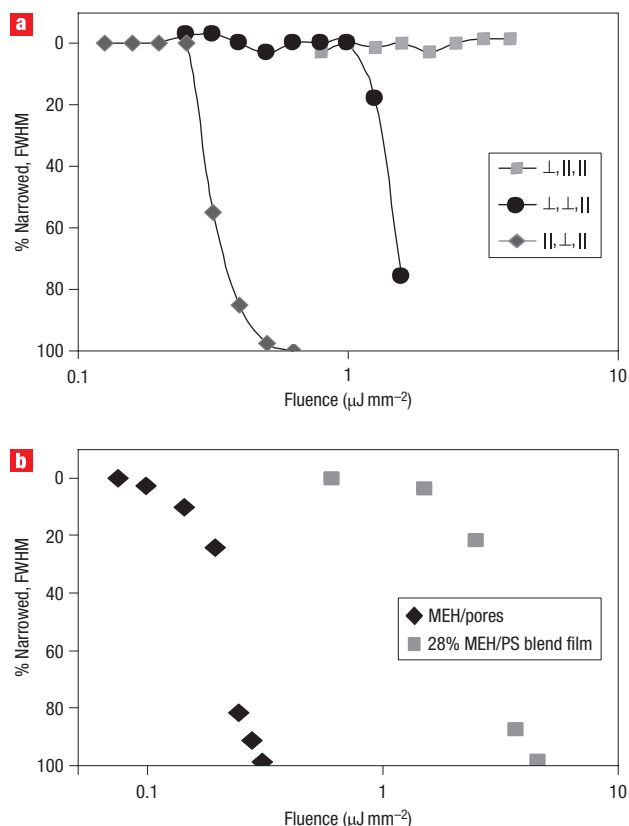


Figure 3 The threshold for ASE depends on both the excitation polarization and the nanoscale alignment of the polymer. **a**, The ASE threshold of an aligned MEH-PPV/nanoporous silica composite for different polarization conditions following excitation at 500 nm. Narrowing of 100% is defined as the smallest emission linewidth (FWHM) measured with the $\parallel, \perp, \parallel$ polarization combination; 0% narrowed is defined as the natural emission linewidth following excitation at low intensity, which is the same for all polarization combinations. Optical damage occurred at excitation fluences above $\sim 5 \mu\text{J mm}^{-2}$. **b**, Comparison between the ASE threshold for the $\parallel, \perp, \parallel$ polarization geometry from an MEH-PPV/aligned mesoporous silica composite film (black diamonds) and a 28% w/w MEH-PPV/PS blend film (grey squares) that had the same polarized optical density and overall thickness as the composite sample.

We chose the 28% MEH-PPV/PS blend to ensure the most fair threshold comparison between the spin-cast and composite films—the 28% blend had the same total thickness and twice the OD as the composite film. As the polymer chains in the blend are unoriented, however, the 28% blend has the same polarized absorbance as the oriented composite film, making the effective density of polarized chromophores the same in both samples. The data indicate clearly that despite the fact that the spin-cast film has comparable polarized polymer chromophore density, the ASE threshold for the composite sample is ~ 20 times lower.

To understand the origins of this dramatic lowering of the ASE threshold in the MEH-PPV/silica composites relative to spin-cast films, it is important to determine precisely how the emitted light is confined in the plane of the composite film. A key to understanding this comes from the observation that no line narrowing occurs in any polarization geometry when the samples are held in the air or under vacuum rather than in glycerol. This suggests that the nature of the waveguide is very important to the ASE process. Because the index of refraction of the composite

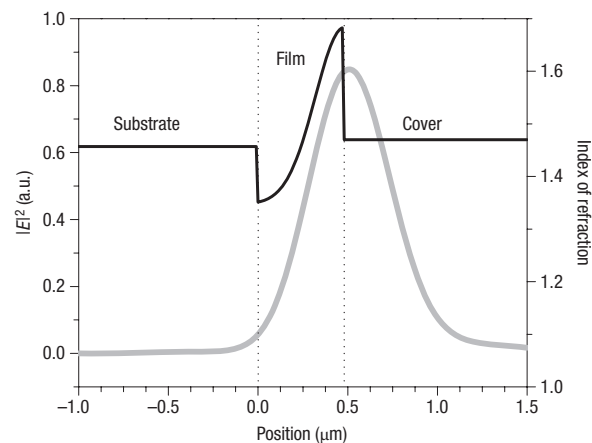


Figure 4 Electric field intensity distribution calculations. The calculated electric field intensity (grey curve) and index of refraction profile (black curve) for a 638-nm emission are plotted along the cross-section of a typical MEH-PPV/aligned mesoporous silica composite film. The calculation demonstrates that the concentration profile produced by diffusive polymer incorporation creates a graded-index waveguide capable of supporting ASE (see text and Supplementary Information for details).

films is a volume-weighted average of the indices of the silica host and the MEH-PPV guest, it appears that the index contrast between the composite film and the substrate and/or cover layer is insufficient to create a waveguide to confine the emitted light in the plane of the film. If the pores are underfilled, however, the polymer distribution is likely to be non-uniform throughout the depth of the film. The polymer concentration gradient in such underfilled composites thus produces an index of refraction gradient, creating a graded-index waveguide that confines light in the plane of the film and allows for ASE if a cover layer with sufficiently high index, such as glycerol, is used.

To better understand how the index gradient from non-uniform incorporation allows the creation of a waveguide, Fig. 4 shows electric-field intensity distribution calculations²² for a typical 480-nm thick composite film (see Supplementary Information for details). We assumed that the spatial distribution of the incorporated MEH-PPV chains was Gaussian, with the maximum polymer concentration at the exposed surface, as expected for diffusive incorporation. We chose the gaussian width of 160 nm to reproduce a typical film's experimentally measured OD of ~ 0.45 , which indicates that $\sim 42\%$ of the pores are filled. We also assumed that the index of refraction of the MEH-PPV chains along the pore direction is 2.40. The black curve in the upper part of Fig. 4 shows the resulting index profile when glycerol ($n = 1.47$) is chosen as the cover layer, and the grey curve is the corresponding electric field intensity distribution for 638-nm light, which clearly has a stable guided mode that confines the emission in the composite. As the index of the cover layer is lowered, the electric field distribution moves further into the substrate, until a threshold is reached at which there is no longer a guided mode (see Supplementary Information), consistent with the fact that we observed no ASE from this composite sample when the cover layer was air ($n = 1.00$). Thus, ASE can also be turned off by simply removing the glycerol cover layer to destroy the guided mode. This graded-index structure is a prime example of how simple solution-phase methods can be used to create complex optical structures from self-organized, nanoscale composite materials.

To better characterize this intrinsic graded-index waveguide, we measured the gain and loss for both composite samples and neat spin-cast films of MEH-PPV in a series of experiments using 'stripe' excitation²¹. We found that the loss in the composite films (23 cm^{-1}) is comparable to or lower than that measured for neat MEH-PPV films (27 cm^{-1}). There are two potential reasons for this reduction in loss, both of which stem directly from the nanoscale architecture of the films. First and most importantly, as discussed above, diffusive polymer incorporation into nanometre-sized pores produces a polymer concentration gradient and thus a graded-index waveguide that is not found in spin-cast films. In such a graded-index structure, light is better confined in the plane of the film (compare with Fig. 4), as compared with a conventional planar waveguide where a significant evanescent wave extends beyond the boundaries of the active layer, creating losses by scattering and absorption in the media immediately adjacent to the film. Second, it is also possible that reducing the size of polymer domains down to a few nanometres reduces scattering losses. Although semiconducting polymers are often treated as homogeneous optical media, a variety of studies indicate that there are clearly domains in these films, and the length scale is usually in an optimal range to scatter visible light^{23,24}.

In addition to changes in the loss, our experiments show that the gain in pure MEH-PPV films is not much higher than the gain in the composite material (54 cm^{-1} versus 43 cm^{-1}), despite the fact that the polarized chromophore density in the pure films is ~ 3.6 times higher than in the composite, and that the gain should scale exponentially with chromophore density²⁵. The relative improvement in gain in the pure MEH-PPV film is thus smaller than that expected from an exponential dependence on OD. This result stands in contrast to previous studies of stretch-aligned conjugated polymer films, which found that the ASE threshold scaled directly with the effective change in chromophore density upon going from randomly ordered to aligned chains²⁶. We believe that the dramatic improvement in gain in the composites stems largely from the graded-index waveguide structure, which provides a more optimal guided mode and thus increases the electric field strength in the active layer of the composite film relative to that in both neat and blended spin-cast polymer films. It is possible that the fact that the ASE threshold of the composite samples is ~ 20 times lower than that of the 28% w/w blended spin-cast film (Fig. 3b) results partially from the fact that blended spin-cast films have additional optical loss from scattering due to phase-segregation of the MEH-PPV in the PS matrix. Previous studies, however, suggest that blending conjugated polymer chromophores in PS affects only the gain due to dilution of the active chromophores (that is, the losses upon blending are roughly constant because spin-cast films are optically flat and phase segregation typically occurs on a length scale much smaller than optical wavelengths; see, for example, ref. 25). In addition, the polymer chains in the composites are not only aligned, but are largely isolated from each other in domains containing only a few polymer chains. This isolation minimizes interchain electronic coupling, which can be detrimental to luminescence and optical gain in spin-cast films^{1,20,27}. Moreover, the straight chain conformation in the composite may also reduce the number of non-radiative defect sites¹³.

The nanometre-scale architecture of these polymer composites thus provides a three-pronged method to improved ASE. First, chain alignment leads to directional, polarized emission. Second, the straight chain conformation and isolation of the chains into nanoscale domains can both improve gain and reduce loss. Finally, the spontaneous formation of a graded-index

waveguide also can both improve gain and reduce loss by maximizing the electric field of the emitted light in the optically active component of the composite and minimizing the field in the substrate. Such films may find applications as secondary emitters in polarized displays, and electrical contact to the aligned polymers in the pores eventually could lead to dramatic advances such as electrically pumped polymer diode lasers.

METHODS

A clean silica glass substrate was coated with polyamic acid, a polyimide precursor, by spin-coating, and then baked at $200\text{ }^{\circ}\text{C}$ for 1 h in air to produce a polyimide film $\sim 10\text{ nm}$ thick. The polyimide film was then rubbed using a nylon-covered cylindrical roller (a buffing wheel) to produce the aligned substrate.

The mesostructured silica film was prepared under hydrothermal conditions through the hydrolysis of silicon alkoxide in the presence of surfactants under acidic conditions. A polyoxyethylene ether nonionic surfactant, Brij56 ($\text{C}_{16}\text{H}_{33}(\text{OCH}_2\text{CH}_2)_{10}\text{OH}$, known as $\text{C}_{16}\text{EO}_{10}$), was used as the template. Tetraethoxysilane ($(\text{C}_2\text{H}_5\text{O})_4\text{Si}$, known as TEOS) was mixed with an acidic solution of $\text{C}_{16}\text{EO}_{10}$, stirred for 2.5 min at room temperature, and then transferred into a Teflon vessel. The molar ratio of the reactant solutions was $0.10\text{TEOS}:0.11\text{C}_{16}\text{EO}_{10}:100\text{H}_2\text{O}:3.0\text{HCl}$. The rubbed substrate described above was held horizontally in the mixture with the rubbed polyimide surface facing downward. To obtain a uniform film, a glass plate was placed $0.2\text{--}0.3\text{ mm}$ from the polyimide surface (Teflon spacers were used to control the solution gap). The vessel was sealed at $80\text{ }^{\circ}\text{C}$ for 5 days to allow for the formation of the mesostructured silica films. These samples were calcined in air to produce porous films. During calcination, the temperature was ramped at $1\text{ }^{\circ}\text{C min}^{-1}$ to $450\text{ }^{\circ}\text{C}$, held for 6 h at $450\text{ }^{\circ}\text{C}$, and then slowly cooled to room temperature.

For semiconducting polymer incorporation, the pore surface was first made hydrophobic by submersion in a 1:1 solution of chlorotrimethylsilane and 1,1,1,3,3,3-hexamethyldisilazane for 2 h. Films were then baked at $200\text{ }^{\circ}\text{C}$ for 2 hours before being rinsed repeatedly in series with chloroform and methanol. The mesoporous silica films were then polymer incorporated by applying approximately 0.1 ml cm^{-2} of a 1% MEH-PPV solution in chlorobenzene onto the centre of the film surface. The films were then placed in a large container with an argon atmosphere and heated at $90\text{ }^{\circ}\text{C}$ for 24 h. Any polymer not incorporated into the pores after heating was dissolved away with chloroform by repeated rinsing.

Received 21 May 2007; accepted 16 August 2007; published 16 September 2007.

References

- Schwartz, B. J. Conjugated polymers as molecular materials: How chain conformation and morphology influence energy transfer and interchain interactions. *Annu. Rev. Phys. Chem.* **54**, 141–172 (2003).
- Miller, E. K., Yoshida, D., Yang, C. Y. & Heeger, A. J. Polarized ultraviolet absorption of highly oriented poly(2-methoxy,5-(2'-ethyl)-hexyloxy paraphenylene vinylene). *Phys. Rev. B* **59**, 4661–4664 (1999).
- Wu, J., Gross, A. F. & Tolbert, S. H. Host-guest chemistry using an oriented mesoporous host: alignment and isolation of a semiconducting polymer in the nanopores of an ordered silica matrix. *J. Phys. Chem. B* **103**, 2374–2378 (1999).
- Hide, F. *et al.* Semiconducting polymers: a new class of solid-state laser materials. *Science* **273**, 1833–1836 (1996).
- Yanagisawa, T., Shimizu, T., Kuroda, K. & Kato, C. The preparation of alkyltrimethylammonium-kanemite complexes and their conversion to microporous materials. *Bull. Chem. Soc. Jpn* **63**, 988–992 (1990).
- Kresge, C. T., Leonowicz, M. E., Roth, W. J., Vartuli, J. C. & Beck, J. S. Ordered mesoporous molecular sieves synthesized by a liquid-crystal template mechanism. *Nature* **359**, 710–712 (1992).
- Yang, H., Kuperman, A., Coombs, N., Mamiche-Afara, S. & Ozin, G. A. Synthesis of oriented films of mesoporous silica on mica. *Nature* **379**, 703–705 (1996).
- Lu, Y. F. *et al.* Continuous formation of supported cubic and hexagonal mesoporous thin films by sol-gel dip-coating. *Nature* **389**, 364–368 (1997).
- Miyata, H. & Kuroda, K. Formation of a continuous mesoporous silica film with fully aligned mesochannels on a glass substrate. *Chem. Mater.* **12**, 49–54 (2000).
- Miyata, H., Kawashima, Y., Itoh, M. & Watanabe, M. Preparation of a mesoporous silica film with a strictly aligned porous structure through a sol-gel process. *Chem. Mater.* **17**, 5323–5327 (2005).
- Molenskamp, W., Miyata, H. & Tolbert, S. H. Highly-polarized luminescence from optical-quality films of semiconducting polymers aligned within oriented mesoporous silica. *J. Am. Chem. Soc.* **126**, 4476–4477 (2004).
- Nguyen, T.-Q., Wu, J., Doan, V., Schwartz, B. J. & Tolbert, S. H. Control of energy transfer in oriented conjugated polymer/mesoporous silica composites. *Science* **288**, 652–656 (2000).
- Cadby, A. J. & Tolbert, S. H. Controlling optical properties and interchain interactions in semiconducting polymer by encapsulation in periodic nanoporous silicas with different pore sizes. *J. Phys. Chem. B* **109**, 17879–17886 (2005).
- Wan, Y., Yang, H. F. & Zhao, D. Y. Host-guest chemistry in the synthesis of ordered nonsiliceous mesoporous materials. *Acc. Chem. Res.* **39**, 423–432 (2006).

15. Huo, Q., Margolese, D. I. & Stucky, G. D. Surfactant control of phases in the synthesis of mesoporous silica-based materials. *Chem. Mater.* **8**, 1147–1160 (1996).
16. Nguyen, T.-Q., Wu, J., Tolbert, S. H. & Schwartz, B. J. Control of energy transport in conjugated polymers using an oriented mesoporous silica matrix. *Adv. Mater.* **13**, 609–611 (2001).
17. Tessler, N., Denton, G. J. & Friend, R. H. Lasing from conjugated-polymer microcavities. *Nature* **382**, 695–697 (1996).
18. McGehee, M. D. *et al.* Semiconducting polymer distributed feedback lasers. *Appl. Phys. Lett.* **72**, 1536–1538 (1998).
19. Wudl, F. *et al.* Polymers and an unusual molecular crystal with nonlinear optical properties. *ACS Symp. Ser.* **455**, 683–686 (1991).
20. Nguyen, T.-Q., Martini, I. B., Liu, J. & Schwartz, B. J. Controlling interchain interactions in conjugated polymers: The effects of chain morphology on exciton–exciton Annihilation and aggregation in MEH-PPV films. *J. Phys. Chem. B* **104**, 237–255 (2000).
21. McGehee, M. D. *et al.* Amplified spontaneous emission from photopumped films of a conjugated polymer. *Phys. Rev. B* **58**, 7035–7039 (1998).
22. Wang, L. & Huang, N. Index profiles: TE mode solutions. *IEEE J. Quant. Electron.* **35**, 1351–1353 (1999).
23. Schaller, R. D. *et al.* Nanoscopic interchain aggregate domain formation in conjugated polymer films studied by third harmonic generation (THG) near-field scanning optical microscopy (NSOM). *J. Chem. Phys.* **117**, 6688–6698 (2002).
24. Schaller, R. D. *et al.* The nature of interchain excitations in conjugated polymers: Spatially-varying interfacial solvatochromism of annealed MEH-PPV films studied by near-field scanning optical microscopy (NSOM). *J. Phys. Chem. B* **106**, 9496–9506 (2002).
25. Diaz-Garcia, M. A. *et al.* Plastic lasers: Semiconducting polymers as a new class of solid-state laser materials. *Synth. Met.* **84**, 455–462 (1997).
26. Heliotis, G. *et al.* Investigation of amplified spontaneous emission in oriented films of a liquid crystalline conjugated polymer. *Synth. Met.* **139**, 727–730 (2003).
27. Martini, I. B., Smith, A. D. & Schwartz, B. J. Evidence for the direct production of interchain species in conjugated polymer films: The ultrafast stimulated emission and fluorescence dynamics of MEH-PPV. *Phys. Rev. B* **69**, 035204 (2004).

Acknowledgements

This work was supported by Canon (S.H.T. and H.M.), by the Office of Naval Research under grant N00014-04-1-0410 (S.H.T. and B.J.S.), and by the National Science Foundation under grants DMR-0305254 (BJS) and CHE-0527015 (B.J.S. and S.H.T.).

Correspondence and requests for materials should be addressed to S.T. or B.J.S.

Supplementary information accompanies this paper on www.nature.com/naturenanotechnology.

Reprints and permission information is available online at <http://npg.nature.com/reprintsandpermissions/>